DOI 10.5162/ETTC2024/A5.2

Comparing FBG Sensors with Electrical Strain Gauges on a Helicopter Rotor Blade during Whirl Tower Test

Simone Weber[1], Raphael Rammer[1], Valerio Camerini[2], Maxime Asselin[2], Florian Kurfiss[1], and Benedikt Köhr[1]
[1]Airbus Helicopters Deutschland GmbH, Industriestr. 4, 86607 Donauwörth, Germany,
[2] Airbus Helicopters S.A.S., Marseille Provence International Airport, France
simone.weber@airbus.com

Abstract:
Fibre Bragg grating strain sensors and conventional electrical strain gauges were deployed on an Airbus Helicopters H145 rotor during a dedicated whirl tower test to examine the accuracy of the optical fibre sensors. Data was streamed wirelessly from the rotor hub-mounted sensor interrogator to a ground station. Changes in strain and vibration signatures in response to a sequence of controlled hydraulic actuator inputs were successfully identified and the parameters of interest of both sensing solutions compared against each other. The outcome of this work demonstrates the potential of using optical fibre sensors for flight testing and providing in-service operational data on helicopter blade dynamics.

Key words: Fibre Bragg grating sensors, optical fibre sensors, electrical strain gauges, helicopter rotor blade, helicopter blade dynamics.

Introduction

Electrical strain gauges (SG) have been used for the measurement of aircraft structural loads for more than 70 years [1,2]. Some reports highlight the deployment of SG in the late 1970s to measure in-flight rotor blade loading in hover and forward flight conditions of a Boeing CH-47A [3,4]. Work conducted in the 1980s adopted a combination of SG and pressure sensors to predict the aerodynamic loading and rotor blade structural deformation for the hover case and for a variety of forward speeds on a Puma helicopter [5]. However, methods using SG have numerous disadvantages. These range from operational limitations, such as high sensitivity to precipitation to long installation times due to tedious wiring of each sensor. Moreover, the large amount of wiring interferes with the aerodynamic and dynamic behaviour of the blade and it is not uncommon that SGs fail during the testing. Robust and reliable measurement of rotating blade deformation is challenging and the search for new non-intrusive measurement techniques have been the subject of numerous studies. While imaging approaches have been trialled in wind tunnels and on whirl rigs [6], their in-flight use is hampered by the large observation angle and depth of field required to measure along the entire length of the blade, along with issues related to background light and to the fouling of the blade surface. Optical fibre-based approaches with optical fibre Bragg gratings (FBGs) have the potential to meet both the measurement requirements and the demands of the measurement environment, with recent reports of their deployment on rotorcraft components in laboratory conditions [7-9], and under flight, or flight-equivalent, conditions [10–15]. In [10], surface-mounted FBG sensors were utilised to monitor the strains on a rotor blade during take-off, a low altitude hover, and landing, using six sensors connected to a battery powered interrogator, with the data logged locally for later processing. The data was post-processed to provide information on the flap, lead-lag and torsion deformation. Recently, as part of the BladeSense programme [11], two optical fibre-based sensing techniques were deployed on the rotor blades of an Airbus Helicopters H135: optical fibre FBG and fibre segment interferometry-based direct fibre optic shape sensing, live-streaming data during a series of ground runs with controlled pilot inputs. Aspects of the work and the findings have been presented previously [12-14], where it was shown that both sensing approaches were capable of detecting the 1/rev rotation frequency, and its harmonics, and of detecting some of the operational modes excited by specific pilot inputs. To increase the acceptance of optical fibre sensors in the aerospace

industry, they need to be benchmarked against SGs. In a previous study a good agreement with a maximum error of 1.8% was achieved during real flight that compared measured dynamic strains of SGs and FBGs on a rotor blade [15].

The work done in this paper focuses on determining the accuracy and reliability of FBG strain sensors compared to conventional SGs during a dedicated whirl tower test on an Airbus Helicopters H145 rotor applying a sequence of controlled hydraulic actuator inputs for rotor load determination and identification of modal properties. Outcome of the test campaign is presented with a clear recommendation for the potential use of optical fibre sensors for flight testing.

Sensors and instrumentation

Three FBG sensor arrays were applied to the flexbeam of the bearingless main rotor of an Airbus Helicopters H145, each containing 4 wavelength-division multiplexed FBGs in Ormocer coated 125µm single mode optical fibres, with the sensors distributed along a 0.4m length of the fibre. The FBG sensor arrays were bonded to the upper and lower surfaces of the flexbeam (see Fig. 1) using adhesive AE10, while Gagekote #8 was applied on top of the FBG as a first protective layer. The entire length of each fibre optic cable was covered with Silicone 3140 RTV to protect the fibres from detaching. Standard electrical SG instrumentation was deployed as a reference during the test campaign. It was ensured that the FBGs were located as close as possible to the SGs despite limited available space due to the required wiring of each single SG on the flexbeam structure. The SGs form a full bridge configuration, meaning they are arranged symmetrically around the neutral axes, similar to the set-up presented in Fig. 1(b). The different sensor locations are depicted in Fig. 1(a) showing the positions of the SGs and the fibre sensors that were deployed on the lower surface of flexbeam, with FBGs G1a to G4a on the leading edge and G1b to G4b on the trailing edge. A different fibre array set-up in Fig. 1(b) shows two FBGs on the upper surface and two FBGs on the lower surface. Fig. 1(c) depicts an image of the final instrumented flexbeam highlighting the limited installation space of FBGs G1c to G4c. It should be noted that the FBG sensor positions presented in this paper are the ones that remained functional after the final blade assembly, in which the flexbeam and the pitch control cuff were merged together. As part of repair measures FBGs G1c to G4c were glued to the upper and lower surfaces once the rotor blade was fully assembled.

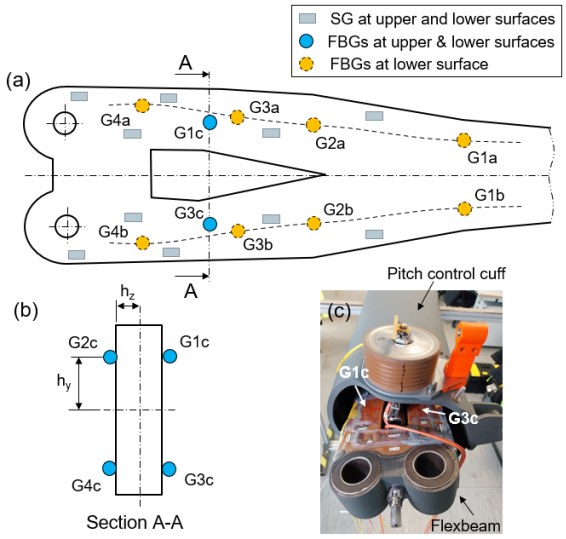

Fig. 1 (a) Diagram depicting positions of the SGs and the fibre sensors deployed on the lower surface of the flexbeam, with FBGs G1a to G4a on the leading edge and G1b to G4b on the trailing edge, (b) only showing fibre sensors mounted on the upper and lower surfaces of the flexbeam with FBGs G1c to G4c, (c) image of the sensor positions G1c and G3c.

The whirl tower test arrangement is presented in Fig. 2. The FBG sensor arrays were interrogated using a 4-channel FBG sensor interrogator mounted on top of the rotor mast, running at a data rate of 2.5 kHz during the whirl tower test campaign. A sampling rate of 0.5 kHz was used for the Airbus internal measurement and control system that allows the determination of bending moments with respect to the SG measurements, calibrated to flap (out-of-plane) and lead-lag (inplane) moments.

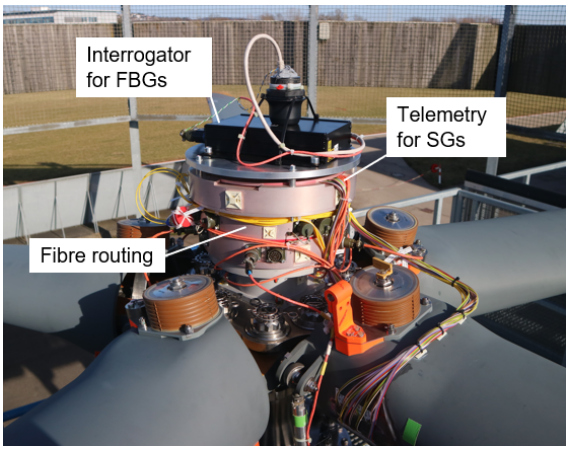

Fig. 2: Whirl tower test: Deployment of FBG strain sensors and electrical SGs with their dedicated data transfer and acquisition devices on an H145 rotor system

In this case, the data transfer from the rotating to the fixed frame was achieved via an inductive Manner telemetry system connected to the

ground station, while the FBG strain sensor data was streamed wirelessly. It was not possible to synchronise the data of the FBGs with the SGs by means of a precision time protocol during the test. Instead, the synchronisation had to be done manually before the data analysis.

Experimental conditions

A whirl tower test was carried out to identify the rotor loads and the modal properties of the main rotor blade, such as natural frequencies and related damping in flap and lead-lag directions. Sufficient excitation of the rotor blade is achieved by providing input with three hydraulic actuators reproducing the collective and cyclic control inputs to the blade via the pitch links (see Fig. 3). The actuators are mounted vertically in the fixed frame of the whirl tower test rig and are located on the same radius around the rotor shaft with an equal spacing of 120°, providing input to the non-rotating part of the swash plate. A cyclic periodic excitation from the actuators to the main rotor is achieved with a sine signal that consists of the same amplitude for all three actuators and a 120° phase shift between the actuators resulting in a 240° phase shift between the first and third actuator. For a steady collective setting all three actuators are moved and fixed in a given position.

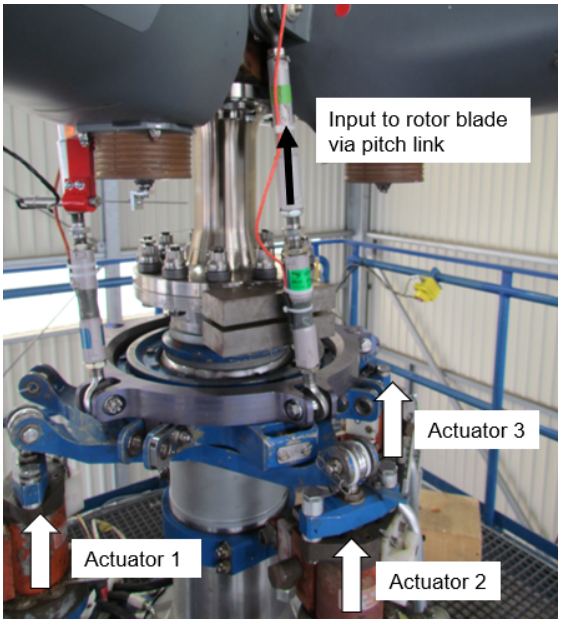

Fig. 3: Actuator arrangement

The required rotor blade loads for flap and lead-lag moment comparison are generated with steady cyclic control inputs, while the excitation of the natural frequencies of the blade is typically achieved with a sine sweep. In case of exciting the flap frequencies of interest as well as the 2nd lead-lag frequency the sine signal is swept within a certain frequency range with one dedicated setting of collective controls and zero cyclic controls. For assessing the 1st lead-lag frequency and associated damping parameters, the same actuator setup was used, but driven at larger amplitudes at a fixed cyclic periodic excitation frequency. This exact value of the input signal was estimated through a short frequency sweep in the range of the estimated lead-lag frequencies. Once a stable condition with large lead-lag moments is obtained, the excitation is stopped instantaneously allowing the identification of frequency and damping of the 1st blade lead-lag mode from measured lead-lag moment decay curves. The same approach is repeated for several steady collective control angles as well as for steady zero and one steady non-zero cyclic control angle.

Results

During the test campaign data totalling around nine hours was collected. While all of the FBG sensors survived the test campaign, one of the SG measurements failed during the whirl tower test. The malfunctioned SG was one of the flap moment measurement positions, which was mounted in a radius range, where large strains occur. This behaviour can often be observed during whirl tower testing or in early flight test phases since the experienced strains at some locations along the flexbeam of a bearingless main rotor are within a range that exceeds fatigue strength of common SGs.

The FBG strain measurements ϵ on opposing sides of the structure were converted to moment to allow a comparison with the SG sensing system that directly outputs bending moments. The flap and lead-lag bending moments, M_{flap} and M_{lag}, are dependent on time t and the radial spanwise location r and are determined as follows:

$$M_{flap}(r,t) = \frac{\epsilon_2(r,t)-\epsilon_1(r,t)}{2\,h_z(r)} EI_{flap}(r) \quad (1)$$

$$M_{lag}(r,t) = \frac{\epsilon_4(r,t)-\epsilon_2(r,t)}{2\,h_y(r)} EI_{lag}(r) \quad (2)$$

for which h_z and h_y are defined as the distance between the neutral axis in vertical and horizontal directions (chordwise), respectively (Fig. 1(b)). EI_{flap} and EI_{lag} are the structural bending stiffness in flap and lead-lag directions. By using strain measurements ϵ on opposing sides, the effect due to temperature, centrifugal loading, and either flap or lead-lag movement is compensated, assuming that the sensors, e.g.

G1c to G4c are on the same spanwise location and arranged symmetrically around the neutral axes.

Since it was difficult to position the FBGs G1c to G4c on the flexbeam surface (refer to Fig. 1(c)) an analysis was performed in which the FBG sensor locations were varied in radial and chordwise locations. The outcome provides some understanding of the effect of positioning errors of ±10 mm on the resulting flap and lead-lag bending moments. As shown in Eq. (1) and Eq. (2) a variation of sensor position in radial direction will alter the values of EI_{flap}, EI_{lag}, and h_z which were modified in accordance with the changing flexbeam geometry, while a deviation in chordwise position influences the value of h_y. Fig. 4 and Fig. 5 present the obtained error on flap and lead-lag moments for different spanwise locations due to the effect of radial and chordwise position deviations, respectively.

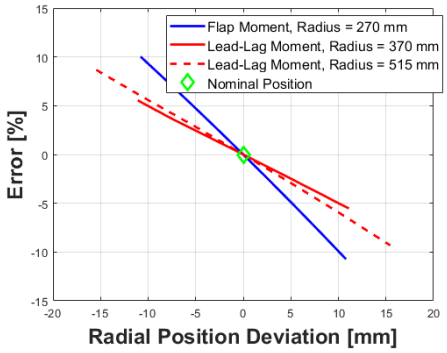

Fig. 4: Resulting error between FBG and SG due to radial position deviation

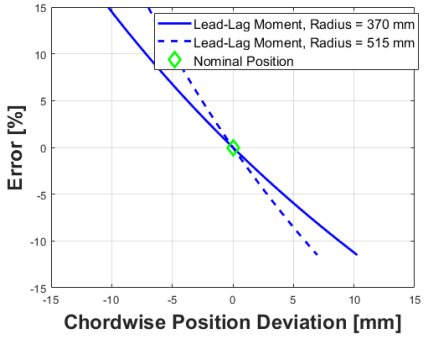

Fig. 5: Resulting error between FBG and SG due to chordwise position deviation

As can be seen in the two graphs, a position error leads to a noticeable difference in the flap and lead-lag moment comparison between both sensing solutions. It should be noted that this is true for both, FBG and SG positioning accuracy. The error due to angular consistency to the blade neutral axis is not considered here, but can lead to further discrepancy within the bending moment comparison.

For the comparison of the flap and lead-lag bending moments a harmonic analysis of the moments, derived from SG and FBG measurements, was performed with an inhouse software. Data without dynamic cyclic excitation was extracted for different collective control angles. The static cyclic control angle was set to approximately 3.4° to introduce a 1/rev loading on the blades. Fig. 6 and Fig. 7 depicts the resulting flap and lead-lag bending moment amplitudes, respectively, determined with the SG and FBG measurements for different collective control angles and sensing positions. The moments determined with FBGs are shown with a ±10 mm sensor variation in radial position and chordwise position, respectively. Additionally, a modal moment distribution for the 1st flap and 1st lead-lag modes was computed and scaled by the mean value of measured 1/rev moments and introduced in the graphs as a reference. Since the scatter from FBGs and SGs around the reference lines exhibit similar behaviour, it is concluded that both sensing solutions deliver similar accuracy for obtained flap and lead-lag bending moments. Possible reasons for such discrepancies are due to the dependency of the SG and FBG sensor positions relative to the neutral axes and subsequently its underlying structural information, needed for the strain to moment conversion. Slight variations of the sensor position will impact the consequential bending moment.

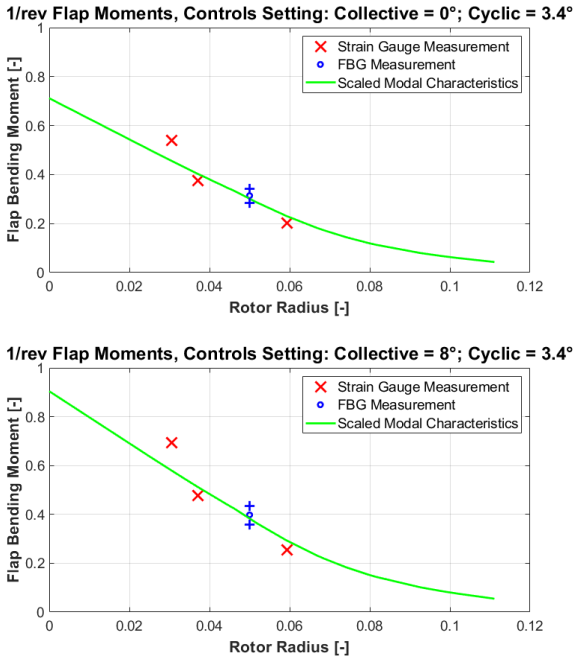

Fig. 6: Flap bending moment comparison, normalised to its maximum moment. The moments determined with FBGs are shown with a ±10 mm sensor deviation in radial position.

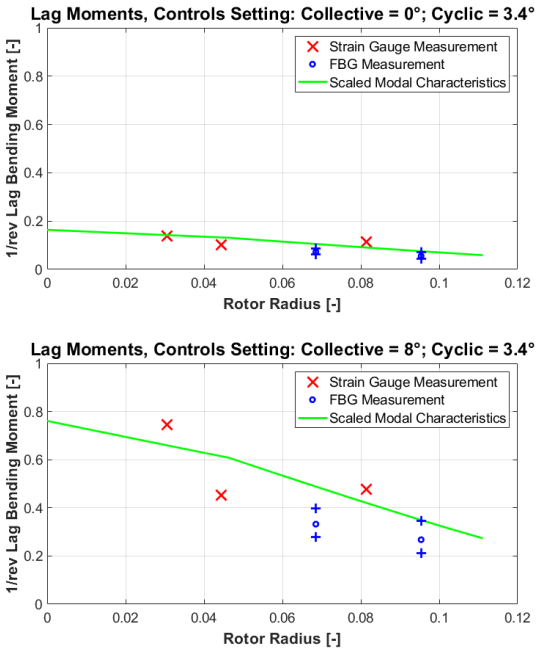

Fig. 7: Lead-lag bending moment comparison, normalised to its maximum moment. The moments determined with FBGs are shown with a ±10 mm sensor deviation in chordwise position.

As for both, FBGs and SGs, no dedicated device apart from measuring tape was applied to position the sensors, a deviation in position and angle from nominal values is very likely. Additionally, as some of the fibres were broken during the flex-control-unit assembly and had to be replaced on the already assembled unit, it was difficult to place the FBG sensors symmetrically around the neutral axes due to stringent space restrictions, see also Fig. 1(c).

For characterising the modal properties the excitation signal from the hydraulic actuators have to be transformed to the rotating frame to create transfer functions of the SG and FBG measurements. Therefore, the measured strokes of the three actuators were transformed to multi-blade-coordinates. By means of the rotor turn marker and rotor speed measurements, the excitation in the fixed frame was transformed to individual-blade-coordinates in the rotating frame. Afterwards, transfer functions were established and evaluated by means of an inhouse software and the natural frequency and damping were identified. Tab. 1 lists the error between natural frequency Δf and between the related damping ratio $\Delta\zeta$ obtained with FBG and SG sensors. While the natural frequencies obtained from FBGs and SGs are in very good agreement, with a percentage error of less than 0.6%, the damping ratio exhibited a percentage error of about 80% which were both of the 2nd flap mode. The identification of the damping coefficient is particularly challenging due to its dependency on measurement noise, sensor placement and identification method [16]. While SGs were distributed in radial direction all over the flexbeam and blade, FBG sensors were only available at inboard radial positions at the flexbeam. A better distribution of FBG sensors would significantly improve the identification of the modal properties of the blade.

Tab. 1: Natural frequency Δf and damping ratio $\Delta\zeta$ error of FBG relative to the SG measurements.

Mode	Δf (%)	$\Delta\zeta$ (%)
1st lead-lag	-0.2	1.8
1st flap	Not identified with SG or FBG	
2nd flap	0.6	-79.9
3rd flap	0.0	-11.5
1st torsion	Not identified with FBG	
2nd lead-lag	0.0	-11.1
4th flap	0.2	0.0

Summary

Fibre optic cables with integrated FBG strain sensors were installed on the surface of the flexbeam with the aim to examine the accuracy of the optical fibre sensors compared to conventionally deployed electrical SG. Data was streamed wirelessly from the rotor hub-mounted sensor interrogator to a ground station.

The determined flap and lead-lag bending moments, as well as modal properties were comparable between FGB and SG sensors with a percentage error of less than 0.6% for the natural frequencies and a percentage error of about 80% for the related damping that was subject to the specific FBG sensor position which was not ideal for identifying this particular mode. Since both sensing systems exhibit a dependency on their position relative to the neutral axes of the flexbeam, a full characterisation of the flap and lead-lag modal properties require careful consideration of sensor location in the chordwise and radial directions. It was also demonstrated that a slight deviation of FBG sensor position in radial and chordwise directions can lead to significant errors in the determination of flap and lead-lag moments.

During the test campaign data totalling around nine hours was collected. While all of the FBG sensors survived the test campaign, one of the SG measurements failed during a whirl tower run with higher flexbeam loading. This behaviour from SGs on flexbeams of bearingless main rotors is already known from past experience, since SGs are loaded at or

above their fatigue limit during whirl tower and subsequent flight testing. It is expected that the optical FBGs exhibit a much longer lifetime compared to SG. While the test preparation was carried out according to industry standards it was shown that the FBG sensors have to be handled in a slightly different manner than components equipped with SGs. After the merging of flexbeam and control cuff and application of varnish several fibres were broken and had to be replaced. Due to the limited accessible space once the blade was fully assembled, slight positioning errors were likely.

While key challenges remain in the area of interrogator miniaturisation, robust data transfer from the rotating to the fixed frame and accurate time synchronisation between all acquisition systems, the outcome of this work demonstrates the potential of using optical fibre sensors for flight testing and providing in-service operational data on helicopter blade dynamics.

References

[1] T.H. Skopinski, W.S.J. Aiken, W.B. Huston, “Calibration of strain-gage installations in aircraft structures for the measurement of flight loads,” NACA Report 1178, 1954.

[2] E. Kottkamp, H. Wilhelm, D. Kohl, “Strain gauge measurements on aircraft,” AGARDograph Vol. 7, (160), 1976.

[3] R. Golub, W. McLachlan, “In-flight measurement of rotor blade airloads, bending moments, and motions, together with rotor shaft loads and fuselage vibration, on a tandem rotor helicopter,” Volume I. Instrumentation and in-flight recording system. Technical Report 67-9A, U.S. Army Aviation Materiel Laboratories, Virginia, USA, 1967.

[4] W.J. Grant, R.R. Pruyn, “In-flight measurement of rotor blade airloads, bending moments, and motions, together with rotor shaft loads and fuselage vibration, on a tandem rotor helicopter,” Volume II. Calibrations and instrumented component testing. Technical Report 67-9B, U.S. Army Aviation Materiel Laboratories, Virginia, USA, 1967.

[5] J. Riley, G.D Padeld, J. Smith, “Estimation of rotor blade incidence and blade deformation from the measurement of pressures and strains in flight,” 14th European Rotorcraft Forum, Milano, Italy, 1988.

[6] F. Boden, B. Stasicki, K. Ludwikowski, “Optical Rotor-Blade Deformation Measurements using a Rotating Camera,” The European Test and Telemetry Conference, 147–154 (2018), doi:10.5162/ettc2018/7.4

[7] S. Weber, T. Kissinger, E. Chehura, S. Staines, et al., “Application of fibre optic sensing systems to measure rotor blade structural dynamics,” Mechanical Systems and Signal Processing, 158, 107758 (2021).

[8] M. Hajek, S. Manner and S. Susse, “Blade root integrated optical fiber Bragg grating sensors a highly redundant data source for future HUMS,” American Helicopter Society 71st Annual Forum Proceedings, Virginia Beach, Virginia, USA, May 2015.

[9] F. Berghammer, B. Sosa, V. Heuschneider, I. Yavrucuk, “Testing of a Fiber-Optical Sensor System for Rotor Blade HUMS,” Vertical Flight Society’s 79th Annual Forum & Technology Display, West Palm Beach, Florida, USA, May 2023.

[10] J. Serafini J, G. Bernardini, L. Mattioni, V. Vezzari, C. Ficuciello, “Non-invasive dynamic measurement of helicopter blades,” J. Phys.: Conf. Ser. 882, 012014 (2017).

[11] S. Weber, D. Southgate, K. Mullaney, S.W. James, et al., “BLADESENSE – A novel approach for measuring dynamic helicopter rotor blade deformation,” 44th European Rotorcraft Forum, Delft, The Netherlands, September 2018.

[12] S. W. James, T. Kissinger, S. Weber, K. Mullaney, et al., “Fibre-optic measurement of strain and shape on a helicopter rotor blade during a ground run: 1. Measurement of strain,” Smart Materials & Structures, Vol. 31, (7), 075014 (2022), DOI 10.1088/1361-665X/ac736c.

[13] S. W. James, T. Kissinger, S. Weber, K. Mullaney, et al., “Fibre-optic measurement of strain and shape on a helicopter rotor blade during a ground run: 2. Measurement of shape,” Smart Materials & Structures, Vol. 31, (7), 075015 (2022), DOI 10.1088/1361-665X/ac736c.

[14] S. W. James, T. Kissinger, S. Weber, K. Mullaney, et al., “Dynamic Measurement of Strain and Shape on a Rotating Helicopter Rotor Blade: The Measurement Challenge,” 28th International Conference on Optical Fiber Sensors, Hamamatsu, Japan, November 2023.

[15] H. Zhang, Z. Wang, F. Teng, P. Xia, “Dynamic Strain Measurement of Rotor Blades in Helicopter Flight Using Fiber Bragg Grating Sensor,” Sensors, 23, 6692 (2023).

[16] X. Wang, K. Liu, H. Liu, Y. He, “Damping Identification with Acceleration Measurements Based on Sensitivity Enhancement Method”, Shock and Vibration, Vol. 28, Article ID 6476783, https://doi.org/10.1155/2018/6476783.